Fig. 1 shows low-magnification under-focus XTEM bright images of He-implanted 6H-SiC. In the present study, 1.5×10^{16}, 5×10^{16} and 1×10^{17} $cm^{-2}$are termed as "low dose", "moderate dose" and "high dose", respectively. In the TEM image, the dark contrasts exhibiting dark spots located in the upper and lower interface of the damage band were observed. This dark contrast originates from a high density of stacking faults and lattice strain caused by implantation-induced damage. In the middle of the damage band, no diffraction contrast was observed after annealing at temperatures $\leq$ 800 °C. Besides, the selected-area diffraction patterns taken from the implantation area over ~200 nm of the corresponding samples are shown as insets (see Fig. 1). It can be seen that a ring pattern is exhibited in this area. These results suggest that complete amorphization occurred in the middle of the damage band. In the as-implantation, the images show that the thickness of amorphous layers corresponds to 125 nm in Fig. 1(a), 140 nm in Fig. 1(d) and 167 nm in Fig. 1(g). Through under-focus and over-focus transformation, nanoscale helium bubbles with 1~2 nm in diameter were observed in the deeper zone of the damage band for the moderate and high dose implanted samples. After annealing up to 800 °C, no significantly structural evolution was found in these samples. Only a small zone of recrystallization occurred near the amorphous/crystalline (a/c) interface, and most of the amorphous layer remained. The density and size of helium bubbles observed in the damage band did not change. After annealing at 900 °C, substantial microstructural features changed compared to the cases of the lower annealing temperature. In the insets of Figs. 1 (c), (f) and (i), the selected-area diffraction patterns taken from the damage band exhibit strong Bragg reflections, suggesting a full epitaxial recrystallization of the amorphized layer at annealing temperature 900 °C. It should be noted that besides the diffraction spots corresponding to the (11-20) diffraction pattern from 6H-SiC, the extra spots due to the (011) diffraction pattern from 3C-SiC (marked in the inset, note that the 111 reflections of 3C-SiC are equivalent to the 10-12 and 0006 reflections of 6H-SiC) were superimposed, suggesting that the polycrystalline structures were formed in the damage band. It is consistent with the report of Harada et al.[1]. Besides, helium bubbles grown significantly for the moderate and high dose implanted samples. In parallel, helium bubbles were found in the damage band of the low dose implanted sample.

Reference

[1] S. Harada, M. Ishimaru, T. Motooka, et al., Appl. Phys. Lett, 69(1996)3534.

3 - 13 HRXRD Study of 6H-SiC Implanted With 300 keV He Ions

Du Yangyang

In this paper, samples used are oriented 6H-SiC $<0001>$ surface supplied by the MIT company. They were cut into 10 mm×10 mm×10 mm in size. The 6H-SiC wafers were implanted with 300 keV He ions to a fluence of 1×10^{17} cm^{-2} at 600°C. The implantation experiment was performed at the 320 kV Multi-discipline Research Platform for Highly Charged Ions of the Institute of Modern Physics, Chinese Academy of Sciences (CAS). The 300 keV He ions were implanted into 6H-SiC in vacuum ($\leq2\times10^{-4}$ Pa) and the current density was approximately 0.8 μA/cm². After He implantation, the samples were isochronally annealed at 750 and 1 200 °C for 30 min, respectively, with the GSL1700X high-temperature vacuum sintering furnace in Ar atmosphere.

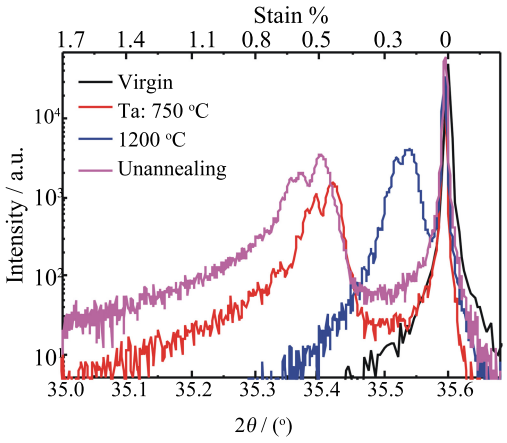

Fig. 1 (color online) Experimental ω-2θ scanning on the (0004) Bragg planes of un-implanted SiC and He-implanted SiC at 600 °C to the fluence of 1×10^{17} cm^2 and subsequently annealed samples at 750 and 1 200 °C for 30 min respectively. The quantity on the top-axis indicates the elastic-strain level. Ta in the figure denotes the annealing temperature.

The HRXRD is a powerful tool for analyzing strains of the near surface caused by ion implantation. The HRXRD measurements were carried out with the D8 Discover HRXRD of BRUKER in the Suzhou Institute of Nano-Tech and Nano-Bionics, CAS. The ω-2θ scanning mode was used near the (0004) Bragg reflection plane with resolution of 0.0001°. A 2 kW sealed X-ray tube was used with pure Cu Kα1 line of wavelength λ=0.154 056 nm and the sample table was equipped with X, Y and Z translational axis and ω, 2θ, ϕ and χ rotational axis.

Fig. 1 shows experimental ω-2θ scanning results. The black curve shows only one main sharp Bragg peak indicating that there is nearly no dilatation of lattice parameter in the direction perpendicular to the material

surface for unimplanted samples. However, new satellite peaks closed to the main Bragg peak for implanted samples appear which are contributed by the diffraction of the near surface region[1]. The crystal near surface strain and the maximum crystal strain can be determined by the positions of the nearest and the farthest new satellite peaks to the sharp main Bragg peak. These strains are shown on the top-axis, and the lower angles correspond to the larger strains. When 6H-SiC wafers were implanted with 1×10^{17} cm^{-2}, the new satellite peak of the closest to the main Bragg peak occurred at lower angles which indicates that significant out-of-plane tensile strain emerged in the near surface of the crystal[2]. With increase of the annealing temperature for the same implanted fluence, the new satellite peak caused by the damage in the near surface area moves towards the larger angle side which indicates that the strain in the near surface region gradually decreases with the increase of annealing temperature. The strain value of implanted-samples can be calculated by the following Bragg equations:

$$2d_1 \sin\theta_1 = n\lambda \ , \tag{1}$$

$$2d_2 \sin\theta_2 = n\lambda \ , \tag{2}$$

where the d_1 , θ_1 and d_2 , θ_2 represent the lattice spacing along c axis and Bragg angles for implanted and unimplanted 6H-SiC respectively. The n and λ stand for the diffraction orders and wavelength of the incident light respectively. We can calculate the strain value ε from Eqs. (1) and (2).

$$\varepsilon = \frac{d_1 - d_2}{d_2} = \frac{\sin\theta_2}{\sin\theta_1} - 1 \ . \tag{3}$$

The near surface strains in He-implanted 6H-SiC as a function of annealing temperatures are shown in Fig. 2. With increase of annealing temperature, the near surface strains gradually decrease. Defects recovery caused by thermal annealing can release the near surface strains. During the process of defects recovery, the migration energies of different point defects such as C vacancies, Si vacancies, C interstitials and Si interstitials play different roles in the near surface strains relaxation. As mentioned in Sawabe et al. work[3], the migration energy of Si vacancy is of the order of 3.2 ∼ 3.6 eV and the migration energy of C vacancy is of the order of 3.5 ∼ 5.2 eV. However, the migration energies of C interstitial and Si interstitial are 0.74 and 1.53 eV, respectively.

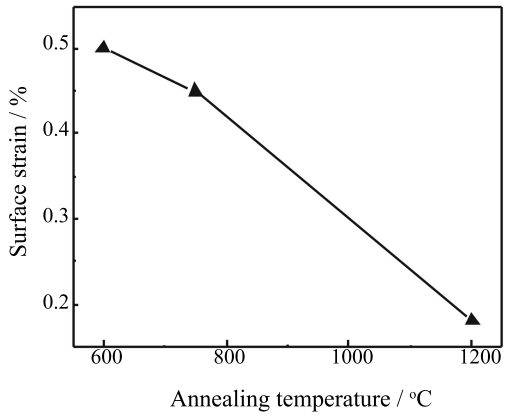

Fig. 2 (color online) The near surface strains in He-implanted 6H-SiC via annealing temperature.

Therefore, Si vacancies and C vacancies start to migrate when the annealing temperature is above 1 273 ∼ 1 473 K and the C interstitials and Si interstitials begin to diffuse above RT and 350 K, respectively[4]. At different annealing stages, the slopes of the curves do not keep constant indicating that different type of defect evolution is responsible for the near surface strains relaxation. When Ta was in the range of 600 to 750 °C, C interstitials and Si interstitials created by He-implantation diffuse and recombine with vacancies thus reducing the defects concentration which releases the near surface strains; When Ta was in the range of 750 to 1 200 °C, Si vacancies and C vacancies also start to migrate and to recombine with mobile C interstitials and Si interstitials that further releases the near surface strains.

Reference

[1] C. L. Xu, C.H. Zhang, J. J. Li, et al., Nuclear Instruments and Methods in Physics Research B, 286(2012)129.

[2] B.S. Li, Z. G. Wang, C. H. Zhang, et al., Journal of Nuclear Materials, 455(2014)116.

[3] Takashi Sawabe, Masafumi Akiyoshi, Kohki Ichikawa, et al., Journal of Nuclear Materials, 386-388(2009)333.

[4] F. Gao W. J. Weber, Journal of applied physics, 94(2004)7.